A Simulation on the Effect of Welding Sequences for T-joints under Single V Groove

Lifei Song, Yunsheng Mao, Zuquan Xiang, Zhuo Chen, Liu Bin
Key Laboratory of High Performance Ships Technology, Ministry of Education (Wuhan University of Technology), Wuhan, China. Email: songlifei@whut.edu.cn, ysmao@163.com, Xiangzuquan@whut.edu.cn, 1304972779@qq.com, 1547628556@qq.com

T-joints are important structural components widely used in the shipbuilding and marine engineering; single V groove is the mostly used groove form for medium-thickness T-joints' welding due to its efficiency. However, because of the asymmetry, complex angular deformation is often produced during welding, which has a negative impact on the structural installation and strength. In this paper, SYSWELD software is used to simulate the welding deformation under single V groove of T-joint based on the thermo-elastic-plastic finite element method. The effectiveness of the model and simulation is verified by experimental results. On this basis, the influence of the welding sequences on the angular deformation is investigated and then the optimal scheme is analyzed. The results provide a theoretical guidance for the practical welding of T-joints in ships and marine engineering structures.

Keywords: Welding Sequence; Angular Distortion; T-joint; Single V Groove

1 Introduction

T-joint is one of the most common welded joints used in the fabrication of structural members in shipbuilding and other similar industries. The welding of T-joints is an essential work, which have an significant impact on subsequent processes. In order to ensure complete penetration and improve the joint strength, it is necessary to carry out bevel cutting in the T-joint before welding. Single V groove is widely used in the welding of medium-thickness T-joints due to its good quality and relatively simple cutting process.

Generally, the welding quality of T-joints, which may cause an undesirable distortions, are mainly affected by unreasonable temperature distribution and residual stresses. To figure out the effect of welding process on different T-joints, researchers have done a lot of work. But due to the complexity of the welding process, early researches are mostly based on experiments. In 1986, Professor Leblond [1] et al. developed the software SYSWELD based on the thermo-elastic-plastic theory to calculate welding residual stress and deformation, which makes it possible to analyze the welding in a modeling and simulation way. Lately, experimentally validated numerical simulations have become a favored method in welding research because of its convenience and efficiency,. Shanmugam, N.S. [2] et al. developed a three-dimensional finite element model (FEM) to analyze the temperature distribution in a laser welding T-joint weld In [3], a linear FEM code withshell elements was put forward to predict weld-induced distortions on combined butt and T-joints. Moreover, the effects of welding factors were also investigated with simulation, and these factors mainly include welding voltage, welding speed, feed rate , gas flow rate[4] and welding method[5]. These literatures mostly focuse on the physical characteristics of T-joints during welding and analyze the effects of different methods and parameters on residual stresses and distortions in welding zone.

Welding sequence is another factor that significantly influence the residual stresses and distortions. Compared with changing welding parameters, it's easier to control since it can be schemed beforehand. Thus the optimization of the welding sequences of T-joints is an important issue that needs to be investigated experimentally and numerically before the structure's construction. A lot of studies about T-joints have been reported in the effect of the welding sequences in recent years. Patek, Marek et al. [5] did the numerical analysis of T-joint welding for bridge construction parts in SYSWELD software and carried out two welding sequences simulations to analyze the changes in residual stresses and final distortions. In [6], a 3D numerical simulation for four welding sequences was carried out to study the varied peak temperatures and the distributions of the vertical and lateral deflections. In [7], Guangming Fu et al. investigated the effect of welding sequence on the residual stresses and distortions in T-joint welds and concluded that the double-side welding procedure induces minimum vertical distortion and relatively smaller residual stress. In [8], an FE model of a Q345D T-joint was established and the welding sequences and direction were considered for reducing the residual deformation and stress, where a symmetrical and 'from the middle to both sides'welding sequence was recommended. R. Keivani et al. [9] investigated the differences of nine welding sequences on distortions and residual stresses in large size T-joints with FEM. And the simulation and experimental results showes that welding sequence influences the peak residual longitudinal stresses at mid-span. In [10], the angular distortions under two welding sequences were studied by Yupiter H.P. Manurung et al. and the results indicate that welding sequence 2 (from outside to inside)get less angular distortion, but in a insignificant way. Park et al. [11] proposed a new model of joint rigidity method to figure out the welding sequence for minimum welding distortion in fabrication for small parts of ships, which was verified by experiment, and the limitations of the algorithm on the complex components were also mentioned. Zargar et al. [12] conducted numerical and experimental study on the effect of submerged arc welding on the residual deformation of fillet welding and verified the feasibility of choosing the

welding sequence by simulation. Faiq et al. [13] optimized the welding sequence of box girder to reduce the welding deformation.

However, most of the reviewed publications focused theoretically on the optimization of welding sequence for general T-joints, which may not be suitable for a specific practical situation. In actual welding of T-joints, as mentioned, there are various types of groove configurations being adopted. For the welding sequences of T-joints with single V groove, which is mostly used in the shiphull section, little work has been reported. hence, The goal of this paper is to figure out the effects of welding sequences on T-joints with single V groove and to find the optimal sequences for practical welding.

This paper is organized as follows: In Section 2, the model and heat source used in this paper are chosen and detailedly stated. Section 3 presents the welding simulation of a T-joint with single V groove; moreover, the temperature, stress and welding deformation along the joint are also analyzed independently. Section 4 gives the experimental results of the T-joint welding, and the simulation and experiment results of angular deformation are compared and analyzed. After that, in Section 5, to optimize the welding sequence, the welding angular deformation of a T-joint with single V groove is analyzed. Finally, a conclusion is given in Section 6.

2 Modeling and heat source verification

The size of the T-joint with single V groove in this paper was as follows: the flange size of 200 × 100 × 12mm, the web size of 100 × 100 × 12mm, the groove angle of 55 °, the root face of 2mm. And the weld consists of the three layers, which are named as bottom layer, filling layer and cover layer.

Marine low-alloy high strength steel Q345 was selected in this study. The heat-physical properties (such as elastic modulus, Poisson's ratio and specific heat capacity) varied with temperature, and partial thermophysical properties at the high temperature were unknown, especially when the steel was in the molten state. Since the welding is a typical highly nonlinear transient process, the properties of the material are obtained with interpolation and extrapolation. Considering the similarity in the thermophysical properties, S355J2G3 was chosen as the welding material in the numerical simulation.

During meshing, we used fine non-uniform grids for the heat affected zone and normal non-uniform grids for the transition zone; while at the other parts away from the weld, the mesh was set gradually sparser so as to improve the calculation rate. Double-ellipsoid heat source model was used for the simulation. By adjusting the shape parameters and the input energy, we obtained a suitable heat source model. The heat density distribution of the heat source in the front half and the rear half are as follow, respectively

$$q_f(\mathrm{x},\mathrm{y},\mathrm{z}) = \frac{6\sqrt{3}(f_f Q)}{a_f bc\pi\sqrt{\pi}} \exp\left(-\frac{3x^2}{b^2} - \frac{3y^2}{a_f{}^2} - \frac{3z^2}{c^2}\right), y \geq 0 \quad (1)$$

$$q_r(\mathrm{x},\mathrm{y},\mathrm{z}) = \frac{6\sqrt{3}(f_r Q)}{a_r bc\pi\sqrt{\pi}} \exp\left(-\frac{3x^2}{b^2} - \frac{3y^2}{a_r{}^2} - \frac{3z^2}{c^2}\right), y < 0 \quad (2)$$

where *af* and *ar* are the length of the front half and the rear half of the double-ellipsoid, respectively; *b* and *c* represent the width and depth of the welding pool, respectively; *q* refers to the heat density inside the material, while *f1*, *f2* are the energy fraction of the front half and the rear half, respectively, where *f1+f2=2*. The welding process parameters are shown in Table 1:

Tab. 1 *The welding parameters for T-joint under single V groove*

Welding layers	Arc voltage U/V	Welding current I/A	Welding speed v/(mm/s)
bottom layer	24	160	5
filling layer	25	180	5
cover layer	24	160	5

3 Simulation results

In the simulation, the welding length of the T-joint with single V groove is 100mm and the welding speed is 5mm/s. We adopt three-layer welding with an overall time of 60s, having a time interval of 10s between two welds. Fig. 1 shows the sampling points used to analyze the temperature distribution of different positions. And the corresponding cross section is chosen as z = -24mm. Node 1 represents the center on the surface of the first layer; node 2 represents the leg on the first layer; node 3 represents a point on the lower surface of the wing plate; node 4 is the intersection of the upper surface of the wing plate and the transition zone, and node 5 is the endpoint of the wing plate.

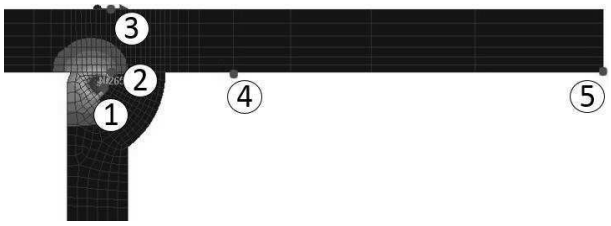

Fig. 1 *The sampling points for thermal cycling analysis*

It can be seen from Fig. 2 that the initial temperatures of the nodes are 20 ℃. Except for node 5, the heating and cooling are conducted three times for these nodes, resulting from the effect of the three-layer welding, and the final temperatures gradually decrease to environment temperature and tend to be stable. Being far from the weld metal area, node 5 is slightly influenced by the heat

source. Comparing the temperature change on different nodes, we can find that the temperature of nodes near the weld zone is strongly influenced by the heat source, which has high heating and cooling rate and changes drastically. While the temperature of the nodes away from the weld zone rises and drops slower and changes in a moderate way.

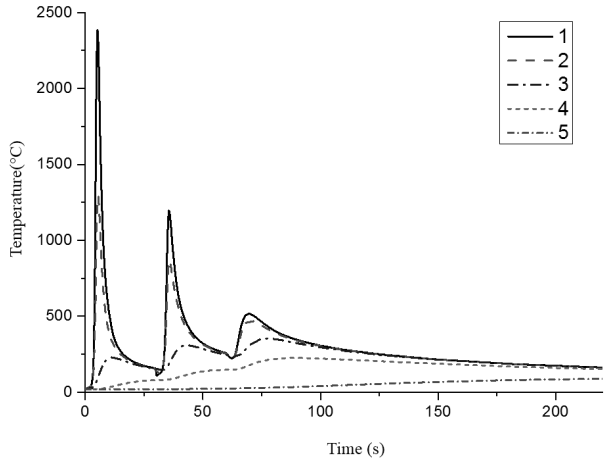

Fig. 2 *The thermal cycling curves of the sampling points*

The Mises stress cloud after the last load step (at 4000s) is shown in Fig. 3.

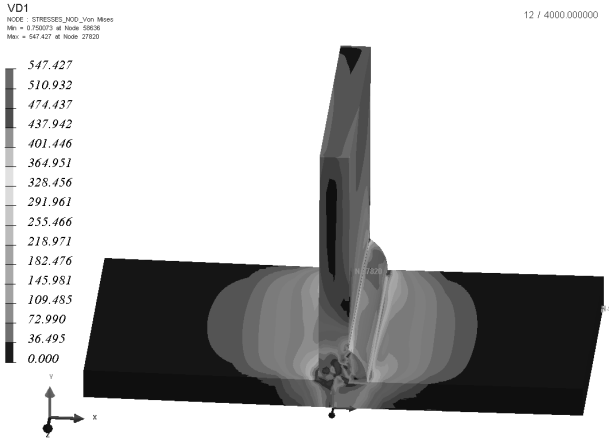

Fig. 3 *The Mises stress distribution under single V groove for the T-joint*

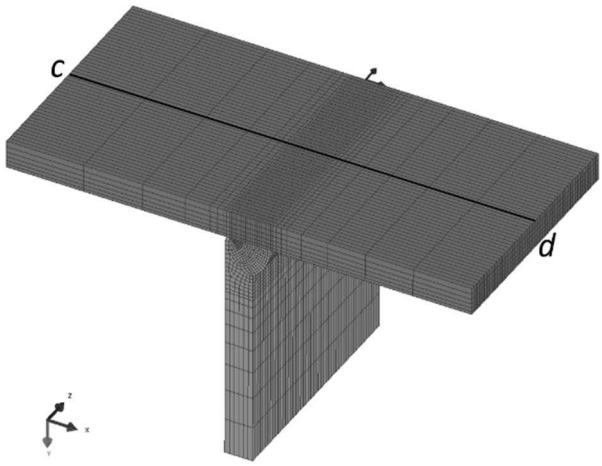

Fig. 4 *A schematic view of path cd*

It can be seen that the residual stress is mainly distributed in the weld zone and the vicinity of the weld, and the distribution area on the right side of the wing is larger than that of the left side, which is caused by different temperature field of the weld arrangement. It is noted that the maximum residual stress near the weld zone reaches 547Mpa, exceeding the yield limit of the material, which indicates a plastic deformation of the material.

After the cooling, the residual stress on the path cd in Fig. 4 is analyzed to obtain the residual stress distribution curve under different X coordinates.

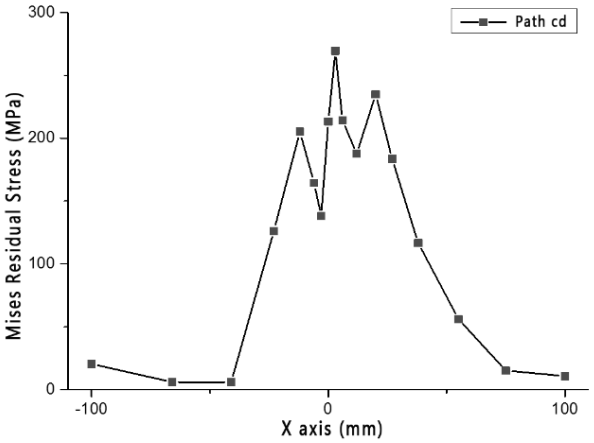

Fig. 5 *The residual stress distribution along the path cd*

In Fig. 5, the distribution curve of the residual stress along the path cd is high and tortuous in the middle, low on both sides; the three peaks of the residual stress appear in the center of the three welds. Moreover, the closer the points to the weld, the larger the residual stress is.

The welding deformation of the T-joint is shown in Fig. 6:

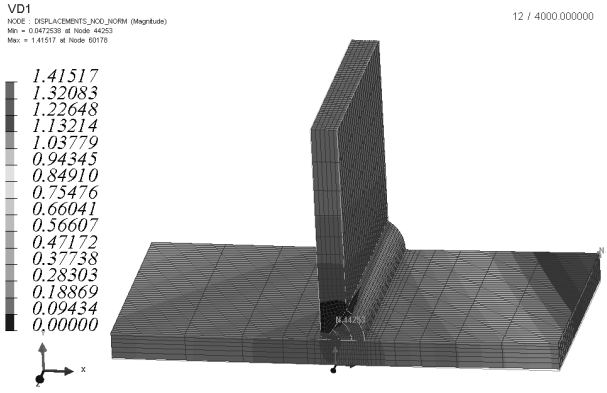

Fig. 6 *Welding deformation clouds for the T-joint with single V groove*

It can be seen from Fig. 6 that the wing plate is warped at both ends, and the major deformation is angular deformation. The maximum angular deformation occurs at the left and right ends of the wing, reaching 0.678013mm and 1.19889mm, respectively; however, the angular deformation on the right side is larger than that of the left. That is mainly caused by the non-uniformity of the weld filling.

As can be seen, the closer the nodes to the weld, the smaller the angular deformation is, which gets a minimum value at the exact center point.

4 Experimental verification

In this part, experimental tests were carried out with a low-alloy high strength steel Q345. Semi-automatic CO2 gas-shielded welding was adopted with welding filler material of ER50-6 and solid wire diameter of 1.2mm. For measurement, we used right angle ruler, vernier caliper and other auxiliary tools. Fig. 7 illustrates the tack welding before welding. The angular deformation of the sampling points was measured and then compared with the numerical simulation results, as Fig 8 shows.

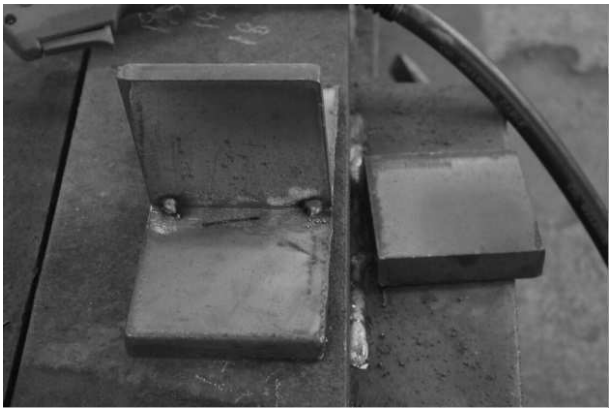

Fig. 7 *The T-joint with single V groove before welding*

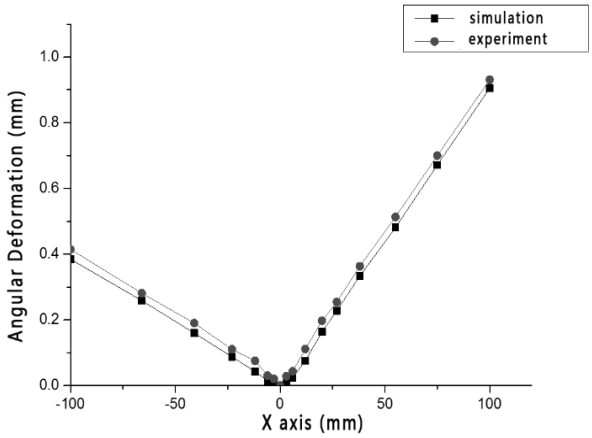

Fig. 8 *Comparison of numerical simulation results and experimental results for angular deformation*

It can be seen from Fig. 8 that the experimental results were consistent with simulation results on the whole, and the little differences between them were explained by following factors:

(1)Numerical simulation error. Since welding is a very complicated process, the numerical simulation can not completely replace the actual welding process, where the simplified heat source model, mesh, material thermal physical properties, boundary conditions and the number of iterations may cause a loss in accuracy.

(2) Measurement error. Due to the limited accuracy of the measuring tool, it's inevitable that certain error is included.

By the above analysis, we can conclude that the numerical simulation method is effective and accurate for welding of T-joints with single V groove. The heat source model we used can be thought to be accurate, which will be later used to study the effect of welding sequence on welding angle deformation of T-joint.

5 Effect of welding sequence on welding angle deformation of T-joint

Considering the structural feature, three schemes for welding sequence were put forward in this paper, as Table 2 shows. And Fig. 9 illustrates the welding paths.

Tab. 2 *Welding sequence schemes*

Schemes	Welding sequence
0 (primitive scheme)	1a-1c，2a-2c，3a-3c
1	1a-1c，2c-2a，3a-3c
2	1b-1a，1b-1c，2b-2a，2b-2c，3b-3a，3b-3c
3	1b-1a，1b-1c，2b-2c，2b-2a，3b-3a，3b-3c

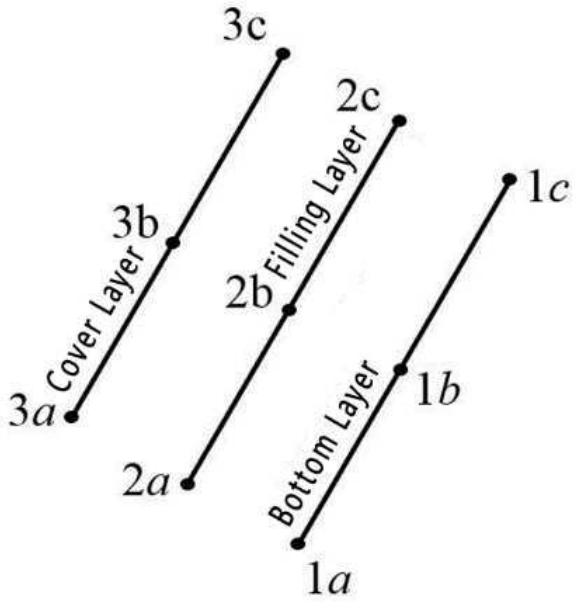

Fig. 9 *A schematic view of the welding path*

From Fig. 1, We chose a point (16mm away from the node 2, Z=-40mm) for analysis. The thermal cycling curves of the four welding schemes (the primitive scheme included) are depicted in Fig. 10.

As can be seen from Fig. 10, the peak temperatures of scheme 1 and the primitive scheme (being subjected to three thermal cycles) are higher than that of scheme 2 and scheme 3 (being subjected to six thermal cycles). And that is mainly due to the fact that each weld in the latter schemes is welded from the middle to both sides, so that the welding heat input is relatively dispersed, which cause

a low peak temperature. Moreover, it's noted that the fourth peak temperature of thermal cycles in scheme 3 is lower than the third peak temperature of thermal cycles in scheme 2. The reason is that the welding direction had switched during the second layer.

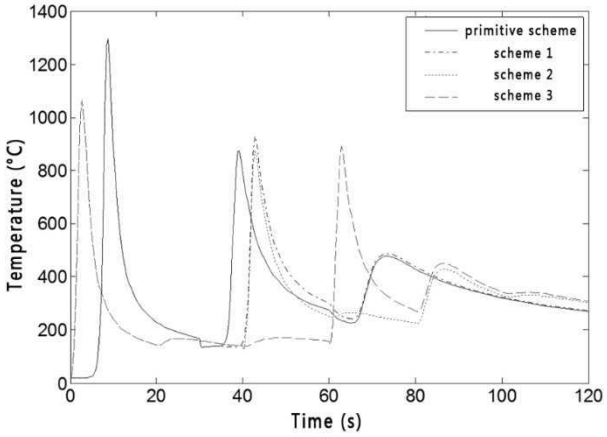

Fig. 10 *Thermal cycling curves of the sampling point under different welding sequence schemes*

The Fig. 11 shows the longitudinal residual stress distribution in path cd under different welding sequence schemes.

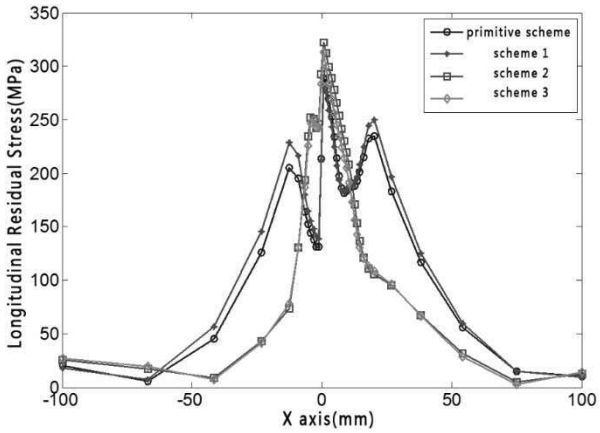

Fig. 11 *Longitudinal residual stress along path cd under different welding sequence schemes*

It can be seen that the residual stress changed most severely in the area of 15mm from the welds, and it was relatively high in the middle and low on two sides. Further, there occurs three peaks along the path cd, which resulting from the effects of the three welds; And the residual stress on the right side is relatively larger than that of the left side, since the weld are mainly arranged on the right side of the joint, resulting in uneven filling and stress distribution. What's more, the longitudinal residual stress in scheme 3 seems to be smallest on the whole, that's because the later welds have a tempering effect on the early ones.

Fig.12 shows the angular deformation along the cd path under different welding sequences. The largest angular deformation of these four schemes all occurred at the both ends of the wing, and the smaller the distance from the weld, the smaller the amount of deformation. It's noted that the angular deformations under the three proposed sequence schemes in descending order are Scheme 3, Scheme 2 and Scheme 1. In Scheme 3, the symmetrical welding is used in each layer, while the order of the symmetrical welding in the adjacent two beads was reversed. In this case, relatively dispersed and the least thermal energy are produced, resulting in the lowest angular deformation.

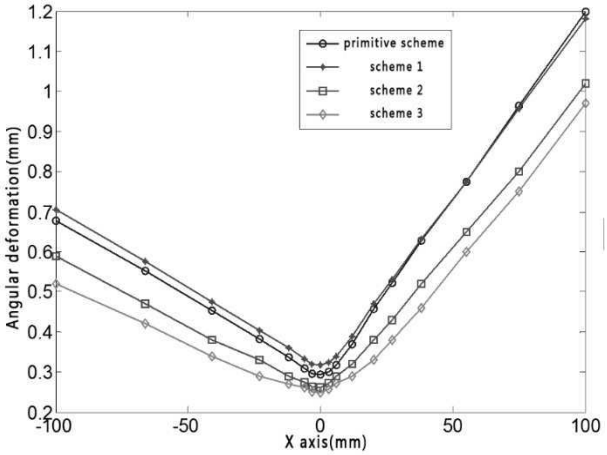

Fig. 12 *Angular deformation along the path cd under different welding sequence schemes*

Based on all the above analysis, we can safely conclude that the temperature field of the T-joint is varied with different welding sequences, which affects the stress field of the components and final angular deformation of the T-joint. And it can be seen that scheme 3, which adopts the symmetrical welding in each layer and opposite welding order between the adjacent two beads, obtains the least heat energy, longitudinal residual stress and angular deformation. Moreover, it can be learned that the angular deformation on two sides of the wing is unevenly distributed, mainly due to the unevenness of the weld filling.

6 Conclusion

In this paper, the influence of the welding sequences on the welding angular deformation of the T-joint with single V groove is studied by combining the simulation and experimental methods. The optimal welding sequence for the groove under the mentioned condition is obtained. In the case of symmetrical welding in each layer and opposite welding order between adjacent two beads, the final residual angular deformation is the lowest. By optimizing the welding sequences, the temperature field of the welding members is changed; the reduced unevenness of temperature change is achieved, the residual stress and the angular deformation after welding are reduced accordingly. And the results can be a reference for practical welding.

Acknowledgements

This Work is supported by the Fundamental Research Funds for the Central Universities under Grants 2017IVA008.

References

[1] LEBLOND, J B., MOTTET, G., DEVAUX, J. C. (1986). A theoretical and numerical approach to the plastic behaviour of steels during phase transformations—II. Study of classical plasticity for ideal-plastic phases [J]. *Journal of the Mechanics & Physics of Solids*, 1986, 34(4):411-432.

[2] SHANMUGAM, N.S., BUVANASHEKARAN, G., SANKARANARAYANASAMY, K., KUMAR, S.R. (2010). A transient finite element simulation of the temperature field and bead profile of T-joint laser welds [J]. *International Journal of Modelling and Simulation*, 2010, 30 (1), pp. 108-122.

[3] MANURUNG, Y. H. P., SULAIMAN, M. S., ABAS, S. K., et al. (2015). Investigation on welding distortion of combined butt and T-joints with 9-mm thickness using FEM and experiment [J]. *International Journal of Advanced Manufacturing Technology*, 2015, 77(5-8):775-782.

[4] KAMBLE, A. G., VENKATA RAO, R. (2016). Effects of process parameters and thermo-mechanical simulation of gas metal arc welding process. *International Journal of Modelling and Simulation*. 2016, 36(4), p 170-182.

[5] LI, C., LIU, L. (2013). Investigation on weldability of magnesium alloy thin sheet T-joints: arc welding, laser welding, and laser-arc hybrid welding [J]. *International Journal of Advanced Manufacturing Technology*, 2013, 65(1-4):27-34.

[6] PATEK, M., MICIAN, M., SLADEK, A., KADAS, D. (2016). Numerical analysis of T-joint Welding with different welding sequences. *Manufacturing Technology*.2016, 16 (1):234-238.

[7] SYAHRONI, N., HIDAYAT, M. I. P. (2011). Numerical Simulation of Welding Sequence Effect on Temperature Distribution, Residual Stresses and Distortions of T-Joint Fillet Welds [J]. *Advanced Materials Research*, 2011, 264-265(5):254-259.

[8] FU, G., LOURENÇO, M. I., DUAN, M., et al. (2016). Influence of the welding sequence on residual stress and distortion of fillet welded structures[J]. *Marine Structures*, 2016, 46:30-55.

[9] SHAO, Q., XU, T., YOSHINO, T., et al. (2017). Multi-objective optimization of gas metal arc welding parameters and sequences for low-carbon steel (Q345D) T-joints[J]. *Journal of Iron & Steel Research International*, 2017, 24(5):544-555.

[10] KEIVANI, R., JAHAZI, M., PHAM, T., et al. (2014). Predicting residual stresses and distortion during multisequence welding of large size structures using FEM[J]. *International Journal of Advanced Manufacturing Technology*, 2014, 73(1-4):409-419.

[11] MANURUNG, Y. H. P., LIDAM, R. N., RAHIM, M. R., et al. (2013). Welding distortion analysis of multipass joint combination with different sequences using 3D FEM and experiment[J]. *International Journal of Pressure Vessels & Piping*, 2013, s 111–112(6):89-98.

[12] PARK, J. U., AN, G. B. (2016). Effect of welding sequence to minimize fillet welding distortion in a ship's small component fabrication using joint rigidity method [J]. *Proceedings of the Institution of Mechanical Engineers Part B Journal of Engineering Manufacture*, 2016, 230(4): 643-653.

[13] ZARGAR, S. H., FARAHANI, M., GIVI, M. K. B. (2015). Numerical and experimental investigation on the effects of submerged arc welding sequence on the residual distortion of the fillet welded plates [J]. *Proceedings of the Institution of Mechanical Engineers Part B Journal of Engineering Manufacture*, 2015, 40(23):31-31.

[14] FAIQ, M., MUFTI, R. A. (2017). Welding sequence optimization for the fabrication of Box Girder[C]// *International Conference on Emerging Technologies*. IEEE, 2017.

10.21062/ujep/129.2018/a/1213-2489/MT/18/3/504